Int. J. Heat Mass Transfer. Vol. 10, pp. 1267–1279. Pergamon Press Ltd. 1967. Printed in Great Britain

ENHANCEMENT OF DIFFUSION-LIMITED VAPORIZATION RATES BY CONDENSATION WITHIN THE THERMAL BOUNDARY LAYER

1. THE CRITICAL SUPERSATURATION APPROXIMATION*

DANIEL E. ROSNER

AeroChem Research Laboratories, Inc., a subsidiary of Ritter Pfaudler Corporation, Princeton, New Jersey

(*Received* 9 *April* 1966 *and in revised form* 8 *March* 1967)

Abstract—The general conditions under which condensation within the thermal boundary layer can enhance the diffusion-limited evaporation rates of liquids or solids in cooler environments are examined analytically, based on the notion that condensation occurs where a "critical supersaturation" is achieved. Simple expressions are derived for the expected enhancement in terms of the dimensionless heat of vaporization Λ/RT_w, the critical supersaturation evaluated at the surface temperature $s_{crit}(T_w) \equiv p_{v,crit}/p_{v,eq}(T_w)$, and a parameter governing the temperature dependence of s_{crit}. These results clearly display the thermodynamic and transport conditions under which large enhancements can be expected. The facility with which they can be used for absolute predictions and comparison with available data is illustrated for the case of molten iron spheres evaporating into quiescent helium at atmospheric pressure.

NOMENCLATURE

a, exponent appearing in equation (21);
A, A', constants [cf., e.g. equation (21)];
b, exponent appearing in equation (21);
B, B', constants [cf., e.g. equation (21)];
B_{diff}, diffusion-limited vaporization ("blowing") parameter, equation (32);
c, local mass fraction of vapor, equation (11);
c_p, specific heat;
D_{v-k}, Fick binary diffusion coefficient for vapor diffusion relative to species k;
Gr, Grashof number [11];
M, molecular weight;
j'', vaporization rate;
J, volumetric nucleation rate;
Le, Lewis number, $D_{v-mix}/[\lambda/(\rho c_p)]_{mix}$;
$\mathscr{L}$, Λ/RT_w;
$\mathscr{N}$, N/RT_w;
Nu, dimensionless transfer coefficient (Nusselt number);
N, parameter defined by equation (2), $A = N/R$ when "log" $\equiv \log_e$;
p, total pressure;
p_v, local vapor pressure;
Pr, Prandtl or Schmidt number [11];
R, universal gas constant;
Re, Reynolds number [11];
$\mathscr{S}$, $s_{crit}(T_w)$;
s_{crit}, critical supersaturation $\equiv (p_v/p_{v,eq})_{crit}$;
T, local absolute temperature;
T_{crit}, thermodynamic critical temperature of substance;
X_k, mole fraction of species k ($k = 1, 2, \ldots$);
Y, dimensionless location of nucleation, equation (7);
y, distance normal to vaporizing surface.

* Revised and extended version of AeroChem TP-130, 31 March 1966. This research was carried out under Contracts AF-49(638)1637 and AF-49(638)1654 with the U.S. Air Force Office of Scientific Research—Propulsion Division.

Greek symbols

- α, evaporation coefficient, cf. equation (22);
- ϵ, evaporation resistance parameter, cf. equation (23);
- δ, effective thickness of the vapor-pressure boundary layer in the absence of condensation, cf. Fig. 1;
- δ_T, effective thickness of the thermal boundary layer, cf. Fig. 1;
- δ_n, effective thickness of the vapor-pressure boundary layer in the presence of condensation, cf. Fig. 1;
- Δ, dimensionless thickness of the vapor-pressure boundary layer in the presence of condensation, cf. equation (9);
- Λ, molar heat of vaporization (or sublimation);
- λ, thermal conductivity;
- ρ, local mass density of vapor–gas mixture;

Subscripts

- crit, critical;
- *eq*, equilibrium;
- max, maximum;
- min, minimum;
- mix, mixture;
- *n*, nucleation;
- *v*, vapor;
- vac, into a vacuum;
- *w*, at wall (vaporizing surface);
- $y = 0$, at wall (vaporizing surface);
- ∞, far from the vaporizing surface;
- λ, pertaining to heat transfer;
- *D*, pertaining to diffusional mass transfer.

1. INTRODUCTION

DIFFUSION-LIMITED vaporization rates of liquids or solids into cooler gaseous media are usually predicted under the assumption that vapor condensation does not occur close enough to the surface to locally modify the vapor concentration profile. This assumption leads to a lower limit to the vaporization rate, since condensation within the thermal boundary layer would provide a vapor "sink" and hence steepen the vapor concentration gradient normal to the surface (i.e. "thin" the vapor concentration boundary layer). This sort of enhancement, in many ways analogous to that produced by chemical reaction within the boundary layer [1, 2], has recently been illustrated by Turkdogan and Mills [3] for the case of induction-heated, molten iron–nickel alloys evaporating into helium. In a companion paper, Turkdogan [4] has proposed a simple model (based on the notion that condensation commences where a critical supersaturation is attained within the thermal boundary layer) which allows the enhancement to be predicted by a graphical technique if certain transport and thermodynamic data are available or estimable. While definitive experiments are apparently not yet available, indications are that this model correctly estimates the magnitude of the observed condensation effect. Unfortunately, while conceptually simple, the numerical–graphical calculations [4] themselves are rather tedious and lack generality. Our purpose here is to cast the critical supersaturation model into a far more transparent and usable form with the help of several reasonable analytical–physical approximations. This new formulation should facilitate future comparisons with experimental data and, perhaps more important, prove helpful in visualizing the conditions under which appreciable enhancements are to be expected. Sufficiently generalized and verified, the present treatment (when "inverted") may even offer a new method for inferring nucleation kinetic data from quasi-steady state vaporation data in, say, "diffusion cloud chambers" (see, e.g. J. L. Katz and B. J. Ostermier, *J. Chem. Phys.*, to be published).

2. THE CRITICAL SUPERSATURATION MODEL

We first confine our attention to the simplest possible case, in which the equilibrium vapor

pressure is established at the vaporizing surface, and this pressure is assumed to be small compared to the total pressure of the system.* We also assume that the heat released upon condensation negligibly perturbs the steady-state temperature distribution near the heated surface. Under these circumstances† the mechanism of condensation-enhanced vaporization can be understood with reference to Fig. 1, which displays actual and hypothetical vapor pressure profiles, $p_v(y)$, in the immediate vicinity of the

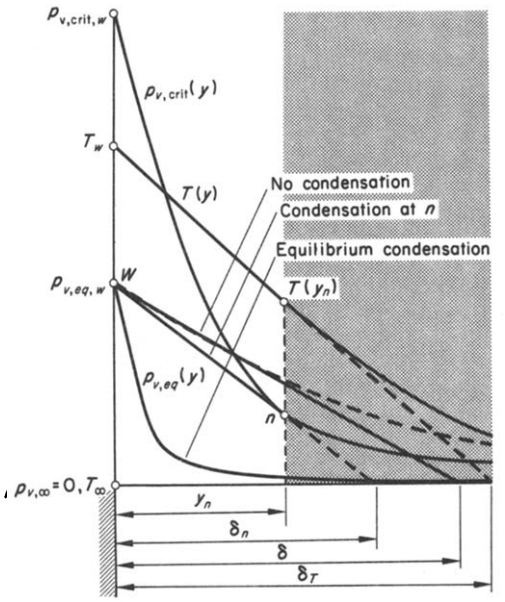

FIG. 1. Temperature and vapor pressure profiles in the immediate vicinity of a vaporizing surface.

surface, as well as the actual temperature profile $T(y)$ established as a result of nonradiative heat loss. Two extreme cases are now readily visualized. In one (shown dashed) condensation does not occur within the thermal boundary layer—this obviously leads to the smallest slope $(-\partial p_v/\partial y)_{y=0}$, and hence the minimum diffusional flux of vapor away from the surface. The second extreme is that in which condensation maintains the local vapor pressure at the thermodynamic equilibrium value $p_{v,eq}(T)$, corresponding to each temperature, $T(y)$, within the boundary layer. As shown below, this leads to a readily calculable upper bound to the evaporation rate, since $(-\partial p_v/\partial y)_{y=0}$ then takes on its maximum possible value. In general, the actual vapor pressure profile will fall between these two extremes and will reflect a balance between the local rate of vapor depletion by nucleation-droplet growth and the net influx of vapor per unit volume by diffusion–convection processes. Moreover, as will be seen [cf. Section 3.4, equation (17)], the wide difference between the maximum and minimum possible vaporization rates (frequently more than one order of magnitude) certainly justifies a rational quantitative treatment of the intermediate case. Unfortunately, calculation of the actual vapor pressure profile entirely "from first principles" is rarely possible or justifiable due to considerable uncertainties in the law governing the local rate of nuclei formation, $J(p_v, T)$, and particle growth, not to mention the many inadequately known property values required as input information [6]. However, it is well established that, at any fixed temperature, $J(p_v, T)$ has the property of being very small until a "threshold" region of $p_v/p_{v,eq}(T)$ is reached, above which nucleation rate is usually too fast to follow experimentally. This property has led to the notion of a "critical supersaturation", $s_{crit} \equiv (p_v/p_{v,eq})_{crit}$, below which the nucleation rate can be neglected.* Since some experimental data on the variation of s_{crit} with temperature are available for vapors of interest, it is reasonable

* Implying that: (i) the nonzero net mass transfer due to vaporization is small enough to have a negligible effect on the temperature and concentration profiles near the surface and, hence, a negligible effect upon the heat- and mass-transfer coefficients [5] and (ii) the thermodynamic and transport properties of the gas mixture are not appreciably influenced by the presence of the vapor.

† Quantitative conditions for the validity of these assumptions are given in Section 4.4.

* In steam turbine practice [7], this property underlies the engineering utility of the so-called "Wilson-line" for estimating the location of condensation on the Mollier (enthalpy vs. entropy) diagram.

to first explore the consequences of this idealization* in predicting enhanced vaporization rates.

If the critical supersaturation ratio, s_{crit}, is known at each temperature $T(y)$, then one can construct the hypothetical vapor pressure profile, $p_{v,\,crit}(y)$, required for nucleation (see Fig. 1), assuming that foreign nuclei are absent in the region of interest.† Vapor fluxes corresponding to values of $(-\partial p_v/\partial y)_{y=0}$ such that $p_v(y)$ does not intersect $p_{v,\,crit}(y)$ are at once ruled out, since the necessary $p_{v,\,crit}$ condition is never achieved. Clearly, the maximum flux compatible with the local attainment of $p_{v,\,crit}$ is that corresponding to the singular case for which the actual vapor pressure profile $p_v(y)$ is also tangent to $p_{v,\,crit}(y)$ at their point of intersection. With regard to the possibility of smaller steady-state fluxes, it seems reasonable to assume that once $p_{v,\,crit}$ has been achieved locally, the nucleation-growth rate is large enough to prevent p_v from exceeding $p_{v,\,crit}(y)$ in the cooler parts of the boundary layer. Since, in the steady state, the vapor flux emerging from the nucleation region cannot exceed that entering (a condition on the change in $\partial p_v/\partial y$ across the nucleation region), these latter two requirements imply that the actual vapor flux will be the maximum compatible with the local attainment of $p_{v,\,crit}(y)$, corresponding to the tangency condition mentioned above and depicted in Fig. 1. This tangency condition, first adopted by Turkdogan [4], simultaneously defines the point n (cf. Fig. 1) at which nucleation "commences" within the thermal boundary layer and thereby determines the actual steady-state vapor pressure gradient $(-\partial p_v/\partial y)_{y=0} = p_{v,\,eq,\,w}/\delta_n$ established in the presence of nucleation-condensation.* By combining available equilibrium vapor pressure and heat-transfer data with quantitative estimates of the required transport properties and critical supersaturation Turkdogan has carried out such calculations graphically for the case of molten iron (and iron–nickel alloy) spheres evaporating into helium. Under the conditions treated ($T_w \approx 2300°K$, $T_\infty \approx 350°K$, $p = 1$ atm), condensation was found to enhance the vaporization rate by a factor of about three (see Section 4.3).

* This is analogous to the "ignition temperature" approximation [8] which proved useful in understanding many properties of combustion waves. In that case the chemical reaction rate was assumed to be negligible below the "ignition temperature".

† This implies that the fluid–particle mechanics in the boundary layer are such as to prevent nuclei or particles formed in the cooler regions of the flow from being swept into the nucleation region considered here in appreciable numbers.

3. GENERAL ANALYTICAL TREATMENT

3.1 *Additional assumptions*

Since the critical supersaturation model outlined above is approximate to begin with, we should not hesitate to introduce further approximations provided they can lead to (i) an appreciable simplification in the computational procedure, (ii) significant insight into the important parameters governing the enhancement and (iii) open the way for further analytical generalizations and extensions of the theory. With these ends in mind, we introduce the following additional assumptions:

(a) The distance y_n to the point of nucleation is small compared with the local radius of curvature of the surface.

(b) The actual temperature profile up to the point of nucleation is linear, with the slope $(\partial T/\partial y)_{y=0}$.

(c) The actual critical supersaturation vs. temperature relation is (locally) well represented by $\log s_{crit} = A \cdot (1/T) + B$ where A and B are constants.

(d) The equilibrium vapor pressure relation is well represented by the Clausius–Clapeyron equation: $p_{v,\,eq}(T) = \text{const} \cdot \exp(-\Lambda/RT)$, where the molar heat of vaporization, Λ, may be considered constant for each substance over the temperature range $(T_w - T_n)$ of interest.

* For simplicity we explicity consider here the case $p_{v,\infty} \ll p_{v,w}$. The present treatment is easily extended to the case when the vapor pressure $p_{v,\infty}$ is not negligible compared with $p_{v,w}$.

Of these assumptions, (a) and (b) (which are self-consistent) are best examined *a posteriori* (cf. Section 4.1), and (d) is known to be accurate; hence, only (c) warrants comment here.

Figure 2 shows Turkdogan's predicted $s_{crit}(T)$ relation for iron vapor (in $\log_{10} s_{crit}$ vs. $1/T$ coordinates). Strong concavity is noted only at temperatures well below the melting point of iron, where the underlying nucleation theory itself becomes uncertain since the relevant nuclei may be solids. Also, if one examines available experimental data and predictions of s_{crit} vs. T for water vapor (summarized in [6]), one again notes that the curvature is slight in log s_{crit} vs. $1/T$ coordinates. In view of the exponential form of the equilibrium vapor pressure relation, (d), this suggests the convenient approximation*

$$s_{crit} = \text{const} \,.\, \exp(N/RT) \tag{1}$$

where† (cf. Fig. 2):

$$N \equiv R\left[\frac{\mathrm{d}(\ln s_{crit})}{\mathrm{d}(1/T)}\right]_{T=T_w} \approx \text{const.} \tag{2}$$

$$\mathcal{N} \equiv N/(RT_w) \tag{4}$$

$$\mathcal{S} \equiv s_{crit}(T_w) = [p_v/p_{v,\,eq}(T_w)]_{crit.} \tag{5}$$

Hence, the enhancement in vaporization rate can be calculated once and for all in terms of these basic parameters.

The tangency condition (cf. Fig. 1) provides the following transcendental equation for the position of nucleation:

$$\frac{1 - \mathcal{S}\exp(\mathcal{L} - \mathcal{N}) \,.\, \exp[-(\mathcal{L} - \mathcal{N})/(1 - Y)]}{\mathcal{S}\exp(\mathcal{L} - \mathcal{N}) \,.\, \exp[-(\mathcal{L} - \mathcal{N})/(1 - Y)]} = \frac{(\mathcal{L} - \mathcal{N})Y}{(1 - Y)^2} \tag{6}$$

where $Y(\mathcal{L} - \mathcal{N}, \mathcal{S})$ is the dimensionless value of y_n, i.e.

$$Y \equiv \frac{y_n}{T_w} \,.\, \left(-\frac{\partial T}{\partial y}\right)_{y=0} = \frac{T_w - T_n}{T_w}. \tag{7}$$

From the value of Y satisfying equation (6) we can then compute the dimensionless form of the thickness δ_n governing $(-\partial p_v/\partial y)_{y=0}$, i.e.

$$\Delta = \frac{(1 - Y)^2}{\mathcal{S} \,.\, (\mathcal{L} - \mathcal{N}) \,.\, \exp(\mathcal{L} - \mathcal{N}) \,.\, \exp[-(\mathcal{L} - \mathcal{N})/(1 - Y)]} \tag{8}$$

3.2 *The tangency condition*

Subject to (a) through (d) one can now analytically formulate the tangency condition displayed in Fig. 1 and solve for the dimensionless value of the thickness $\delta_n \equiv p_{v,\,eq}(T_w)/(-\partial p_v/\partial y)_{y=0}$ in terms of only two dimensionless parameters, viz. $(\mathcal{L} - \mathcal{N})$ and $\mathcal{S}$, where

$$\mathcal{L} \equiv \Lambda/(RT_w) \tag{3}$$

where

$$\Delta \equiv \frac{\delta_n}{T_w} \,.\, \left(-\frac{\partial T}{\partial y}\right)_{y=0}. \tag{9}$$

3.3 *Calculation of the enhanced vaporization rate*

Considering only vapor transport by Fick diffusion, the outward flux of vapor from the

* The Gibbs–Kelvin equation [6, 9] reveals that the validity of this approximation is related to the temperature dependence of both the surface tension (or surface free energy) of the nucleus and its molecular volume. If these physical quantities were temperature independent log s_{crit} would be linear in $1/T^{\frac{3}{2}}$ (see [9]). Interestingly enough, experimental relations similar to equation (1) have proven useful in the description of vapor nucleation on surfaces (see [10]).

† $s_{crit} = 1$ at the thermodynamic critical temperature (or, somewhat reluctantly, rewritten: $s_{crit,\,crit} = 1$!); hence equations (1) and (2) imply that the constant appearing in equation (1) is of the order of $\exp(-N/RT_{crit})$.

surface will be given by

$$j'' = -\left[D_{v-\mathrm{mix}}\,\rho\cdot\left(\frac{\partial c}{\partial y}\right)\right]_{y=0} \tag{10}$$

where c is the local mass fraction of the vapor, given by

$$c \equiv \frac{\rho_v}{\rho} = \frac{M_v}{M_{\mathrm{mix}}}\cdot\frac{p_v}{p}. \tag{11}$$

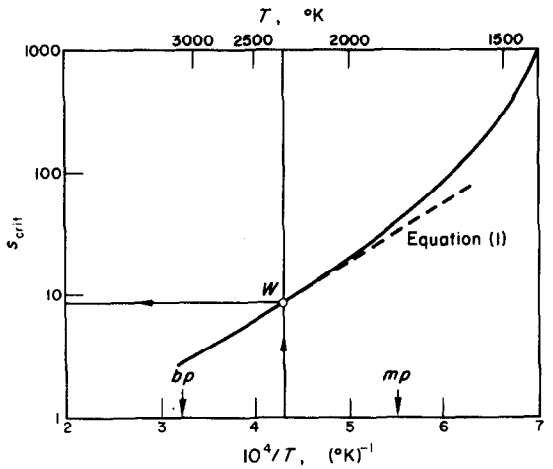

FIG. 2. Predicted critical supersaturation vs. temperature for iron vapor [4] (solid curve); the exponential approximation (dashed).

Consistent with the assumed diluteness of the metal vapor, c is small* so that the mean molecular weight of the mixture, M_{mix}, may be identified with the mean molecular weight of the surrounding gas. Moreover, if the mixture behaves like a perfect gas and $p \approx$ const, then equation (10) can be written explicitly in terms of $(-\partial p_v/\partial y)_{y=0}$:

$$j'' = \left[\frac{D_{v-\mathrm{mix}}M_v}{RT}\left(\frac{-\partial p_v}{\partial y}\right)\right]_{y=0}. \tag{12}$$

Let us denote by $j''_{\min}$ the evaporation rate in the absence of any enhancement, but with all other heat- and mass-transfer conditions the same. Then it is clear from equation (12) that

$$\frac{j''}{j''_{\min}} = \frac{(-\partial p_v/\partial y)_{y=0}}{[(-\partial p_v/\partial y)_{y=0}]_{\min}} = \frac{\delta}{\delta_n} = \frac{\delta}{\delta_T}\cdot\left[1-\frac{T_\infty}{T_w}\right]\cdot\frac{1}{\Delta} \tag{13}$$

where the last equality follows from the definitions of Δ and δ_T (cf. Fig. 1). But in gaseous media, under identical fluid dynamic conditions, the ratio of the ordinary concentration boundary-layer thickness, δ, to the thermal boundary-layer thickness, δ_T, is quite accurately given by the ratio of the heat-transfer coefficient (Nusselt number, Nu_λ) to the mass-transfer coefficient (Nusselt number,* Nu_D) [11]. We thus arrive at the remarkably simple and useful result:

$$\frac{j''}{j''_{\min}} = \frac{Nu_\lambda}{Nu_D}\cdot\left[1-\frac{T_\infty}{T_w}\right]\cdot\frac{1}{\Delta(\mathscr{L}-\mathscr{N},\mathscr{S})} \tag{14}$$

which, according to the present model, applies for conditions such that $(j''/j''_{\min}) \geqslant 1$.

3.4 *Calculation of the maximum possible vaporization rate*

Disregarding equation (14) (for the moment), one can readily obtain an expression for $j''_{\max}/j''_{\min}$ by combining equation with the notion of local thermodynamic equilibrium.† The latter condition implies $p_v(y) = p_{v,eq}[(T(y)]$, hence

$$\left[\left(-\frac{\partial p_v}{\partial y}\right)_{y=0}\right]_{\max} = \left(-\frac{\partial p_{v,eq}}{\partial y}\right)_{y=0} = \left(\frac{\mathrm{d}p_{v,eq}}{\mathrm{d}T}\right)_{T=T_w}\cdot\left(-\frac{\partial T}{\partial y}\right)_{y=0}. \tag{15}$$

* This implies that $D_{v-\mathrm{mix}}$ can be calculated from the relation

$$D_{v-\mathrm{mix}} = \left[\sum_{k\neq v} X_k/D_{v-k}\right]^{-1}.$$

* Often referred to as the Sherwood number in the United States chemical engineering literature.

† In a manner closely related to the treatment of energy transfer in chemically reacting equilibrium gas mixtures [12].

But, from the Clausius–Clapeyron equation (d) we readily find

$$\left(\frac{dp_{v\,eq}}{dT}\right)_{T=T_w} = \frac{p_{v\,eq,w}}{T_w}.\mathscr{L}. \qquad (16)$$

Combining these results we conclude that the maximum possible enhancement is given by:

$$\frac{j''_{max}}{j''_{min}} = \frac{Nu}{Nu_D}.\left[1 - \frac{T_\infty}{T_w}\right].\mathscr{L}. \qquad (17)$$

Comparing this with the more general relation (14) we see that

$$\frac{j''}{j''_{max}} = \frac{1}{\mathscr{L}.\Delta(\mathscr{L} - \mathscr{N}, \mathscr{S})} \qquad (18)$$

from which it is clear that Δ cannot be smaller than $1/\mathscr{L}$. For allowable* values of the critical supersaturation ($\mathscr{S} \geqslant 1$) this is indeed found to be the case (cf. Section 4.1). Physically, the limit $s_{crit} \to 1$ corresponds to the absence of any kinetic limitations on the phase change process; hence, $p_v(y) \to p_{v,eq}[T(y)]$.

4. RESULTS AND DISCUSSION

4.1 *Computation of the dimensionless thickness* Δ

Figure 3 displays the universal function $\Delta(\mathscr{L} - \mathscr{N}, \mathscr{S})$ obtained from equations (6) and (8). Values of Δ read from this plot enable the calculation of actual enhanced vaporization rates in accord with equations (14) and (18). In addition, they can be used to obtain the (dimensionless) position of nucleation within the thermal boundary layer, Y, since equations (6) and (8) reveal:

$$\Delta = Y + [(1 - Y)^2/(\mathscr{L} - \mathscr{N})] \qquad (19)$$

(i.e. Y is only slightly smaller than Δ when $\mathscr{L} - \mathscr{N}$ is large). One notes that small values of Δ (and, hence, large enhancements in vaporization rate) are obtained when the required ("critical") supersaturation at the wall temperature is not large compared to unity, but $\mathscr{L} - \mathscr{N}$ is large. Physically, these conditions are met when the equilibrium vapor pressure drops sharply with a reduction in temperature (i.e. $\mathscr{L} \equiv \Lambda/RT_w$ is large) and when the supersaturation required for nucleation is small (not much larger than unity) and weakly temperature dependent ($\mathscr{N} \equiv N/RT_w$ small). Under these circumstances the present formulation is intrinsically most accurate, since nucleation occurs quite near the surface. Inspection of typical temperature profiles in the vicinity of heated isothermal surfaces reveals that the linear approximation (b) is quite reasonable for $(T_w - T_n)/(T_w - T_\infty) \leqslant \frac{1}{2}$. (See, for example [13] which displays profiles for nonseparated and separated laminar boundary layers, both of which are expressed in terms of the incomplete gamma function.) This implies that the present treatment is self-consistent only if $Y \leqslant \frac{1}{2}[1 - (T_\infty/T_w)]$. For this reason, the function $\Delta(\mathscr{L} - \mathscr{N}, \mathscr{S})$ has been displayed (Fig. 3) only in the (unshaded) region $Y \leqslant \frac{1}{2}$.

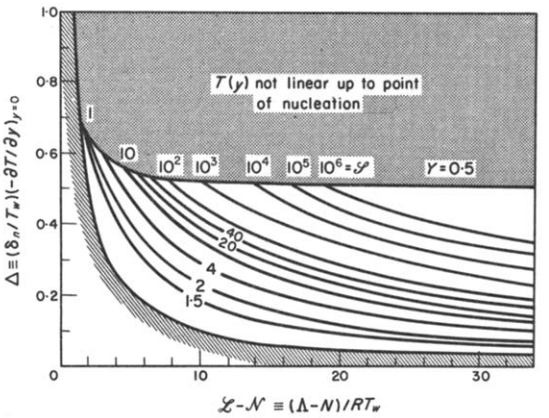

FIG. 3. Modified boundary-layer thickness as a function of vaporization and critical supersaturation parameters (dimensionless).

* Only in the presence of hydrophilic foreign nuclei can condensation be induced at "subsaturations", i.e. "supersaturations" less than unity.

4.2 *Transport conditions favoring large enhancements*

If the diffusivity ratio $Le \equiv D_{v-\mathrm{mix}}/[\lambda/(\rho c_p)]_{\mathrm{mix}}$ were near unity, then, according to the well-known heat–mass transfer analogy [11], the Nusselt number ratio Nu_λ/Nu_D would also be approximately unity. Equation (16) then reveals that condensation within the thermal boundary layer cannot possibly enhance vaporization rates unless the ambient temperature is low enough to satisfy the simple inequality

$$T_\infty \leqslant T_w \cdot [1 - \Delta(\mathscr{L} - \mathscr{N}, \mathscr{S})]. \qquad (20)$$

When $Le \neq 1$, the Nusselt number ratio* Nu_λ/Nu_D will depend on the numerical value of Le (and weakly on the temperature ratio T_∞/T_w, when the latter is significantly less than unity). For configurations described by correlations of the Nusselt power-law form,

$$Nu = A' + B' \cdot (Re \text{ or } Gr)^a (Pr)^b \qquad (21)$$

it is readily shown that Nu_λ/Nu_D must lie between 1 and $(Le)^b$ where the exponent b is typically near $\frac{1}{3}$. It follows that conditions in which the diffusion coefficient $D_{v-\mathrm{mix}}$ exceeds the mixture thermal diffusivity favor larger enhancements. In any particular case, the prevailing ratio Nu_λ/Nu_D is readily estimated from equation (21) for use in equation (14).

4.3 *Application to available vaporization data*

As a start we have applied the present formulation to the experimental conditions recently examined by Turkdogan and Mills [3], viz. diffusion-limited evaporation of inductively heated, molten iron–nickel alloy "spheres" [nominal diameter = 0·64 cm] magnetically levitated in 350°K quiescent helium at atmospheric pressure.

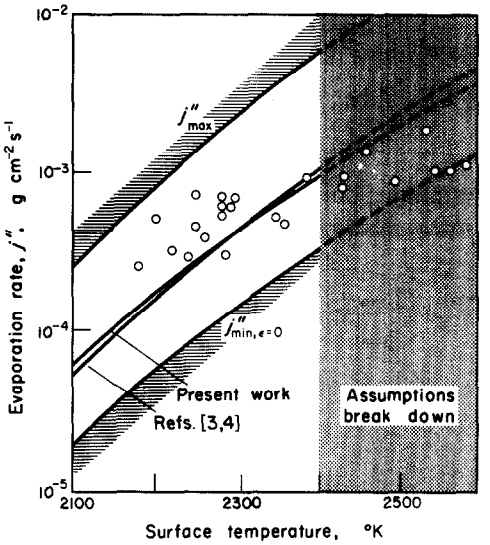

FIG. 4. Predicted and observed vaporization rates for heated, molten, iron spheres in quiescent helium ($p = 1$ atm, $T_\infty = 350$°K, nominal diameter = 0·64 cm).

Figure 4 shows the observed and predicted variations of the average evaporation rate with surface temperature,* together with Turkdogan's graphical prediction [3, 4]. Using the same transport and thermodynamic data† we have also superimposed $j''_{\max}$ as obtained from equation (16). While scatter in the available experimental data precludes a definitive judgement concerning the merits of the critical supersaturation model, at this stage it is noteworthy that (i) the observed vaporization rates fall between the predicted bounds $j''_{\min}$ and $j''_{\max}$ and (ii) the present analytical methods rapidly enable reasonable estimates to be made of the actual enhancements due to nucleation-condensation within the thermal boundary layer. The need

* Strictly speaking, the present analysis holds for local vaporization rates, in which case the transfer coefficients, Nu, appearing in equations (16) and (19) should be local coefficients. Often, however, only average vaporization rates (for an entire surface) are of interest, in which case the theory applies approximately only if the entire surface is isothermal and vaporizing, and one introduces the appropriate average transfer coefficients.

* $j''(T_w)$ predictions have been terminated where the underlying assumptions (no net mass-transfer effect, negligible latent heat effect on temperature profile) become indefensible. These complicating phenomena, discussed in greater detail in Section 4.4, may account for the apparently weaker temperature dependence exhibited by the evaporation data.

† At $T_w = 2300$°K these data led to the values $\mathscr{L} = 18{\cdot}6$, $\mathscr{N} = 4{\cdot}5$, $\mathscr{S} = 8{\cdot}9$, and $Le = 0{\cdot}45$. At 2300°K our predicted enhancement is then a factor of 2·9.

for such methods is evident from the fact that in the present example (cf. Fig. 4) j''_{max} exceeds j''_{min} by more than an order of magnitude. However, data of higher precision, obtained specifically to test the condensation-enhancement mechanism using a convenient experimental system, will be needed to guide future theoretical developments.

4.4 *Further generalizations and discussion of assumptions*

It is desirable to have available quantitative criteria which define the conditions for which the assumptions underlying the present treatment are valid. Ideally, this information would be provided by a more general analysis which includes one or more of the phenomena neglected in the simplest treatment, and thereby allow the errors to be calculated. However, conditions under which the assumptions become too restrictive can also be estimated using simple physical arguments based on the existing analysis. Both approaches are illustrated below.

4.4.1 *Interfacial resistance to evporation.* Relaxation of the assumption $p_{v,w} = p_{v,eq}(T_w)$ well illustrates the value of the present analytical formulation, since this generalization is readily formulated and solved with the introduction of only one additional dimensionless parameter. Moreover, when the effect is small, a perturbation approach provides a simple expression for the magnitude of the $p_{v,w} \neq p_{v,eq}(T_w)$ effect in terms of the solution already presented.

Whenever there is a net flux of vapor, the difference $p_{v,eq}(T_w) - p_{v,w}$ is non-zero and is governed by the evaporation coefficient [14] α appearing in the generalized boundary condition:

$$\left[\frac{D_{v-mix}M_v}{RT}\left(\frac{-\partial p_v}{\partial y}\right)\right]_{y=0} = \frac{\alpha M_v}{4}\left(\frac{8RT_w}{\pi M_v}\right)^{\frac{1}{2}} \cdot \left\{\frac{p_{v,eq}(T_w) - p_{v,w}}{RT_w}\right\}. \quad (22)$$

This boundary condition, which equates the diffusional vapor flux away from the surface to the net vaporization rate provided by the Hertz–Knudsen equation, is readily incorporated into the previous treatment, with the introduction of a single new "evaporation resistance" parameter (dimensionless)

$$\epsilon \equiv \frac{\left[\frac{D_{v-mix}}{T}\left(-\frac{\partial T}{\partial y}\right)\right]_{y=0}}{\frac{\alpha}{4}\cdot\left(\frac{8RT_w}{\pi M_v}\right)^{\frac{1}{2}}}. \quad (23)$$

The tangency condition is found to be identical to equation (6), except for the introduction of the factor $[1 + (\epsilon/Y)]$ on the right-hand side.* In considering the effects of the evaporation resistance parameter on vaporization rates enhancements due to condensation, one must bear in mind that ϵ will also have an effect in the absence of condensation; so it is necessary to distinguish between j''_{min} and $j''_{min,\epsilon=0}$. We find:

$$\frac{j''_{min}}{j''_{min,\epsilon=0}} = \left\{1 + \frac{\epsilon}{(Nu_\lambda/Nu_D)[1 - (T_\infty/T_w)]}\right\}^{-1}. \quad (24)$$

Keeping this distinction in mind, the most convenient generalization of equation (14) becomes:

$$\frac{j''}{j''_{min,\epsilon=0}} = \left\{\frac{Nu_\lambda}{Nu_D}\cdot\left(1 - \frac{T_\infty}{T_w}\right)\cdot\frac{1}{\Delta}\right\}\cdot\left\{1 + \frac{\epsilon}{\Delta}\right\}^{-1} \quad (25)$$

where, now $\Delta = \Delta(\mathscr{L} - \mathscr{N}, \mathscr{S}, \epsilon)$

There is a very simple and useful relationship between the evaporation resistance parameter ϵ, the maximum vaporization rate j''_{max} given by equation (17), and the corresponding rate, j''_{vac}, at which vaporization would occur in a perfect vacuum. Since the latter is given by

$$j''_{vac}(T_w) \equiv \frac{\alpha M_v}{4}\cdot\left(\frac{8RT_w}{\pi M_v}\right)^{\frac{1}{2}}\cdot\frac{p_{v,eq}(T_w)}{RT_w} \quad (26)$$

* The relation between Y and Δ [equation (19)] remains unaltered when $\epsilon \neq 0$.

[obtained by letting $p_{v,w} \to 0$ in the right-hand side of equation (22)], equations (17, 23) and (26) reveal

$$\epsilon = \frac{1}{\mathscr{L}} \cdot \left(\frac{j''_{\max}}{j''_{\text{vac}}} \right). \tag{27}$$

As an example, from this relation and the values of $j''_{\text{vac}}(T_w)$ for Fe(l) given in [4] we readily find that for the evaporation experiment discussed in Section 4·3, $\epsilon = 2{\cdot}7 \times 10^{-3}$ at $T_w = 2300°\text{K}$. This leads to about a 0·4 per cent reduction in the predicted vaporization rate at this temperature and a slightly reduced temperature dependence of $j''(T_w)$ when the effect is included at other temperatures.

When ϵ is small compared to unity, it is reasonable to evaluate the effects of non-zero ϵ by seeking parameter expansions of the form

$$Y(\mathscr{L} - \mathscr{N}, \mathscr{S}, \epsilon) = Y^{(0)}(\mathscr{L} - \mathscr{N}, \mathscr{S}) + \epsilon\, Y^{(1)}(\mathscr{L} - \mathscr{N}, \mathscr{S}) + \ldots \tag{28}$$

$$\Delta(\mathscr{L} - \mathscr{N}, \mathscr{S}, \epsilon) = \Delta^{(0)}(\mathscr{L} - \mathscr{N}, \mathscr{S}) + \epsilon\, \Delta^{(1)}(\mathscr{L} - \mathscr{N}, \mathscr{S}) + \ldots \tag{29}$$

where $Y^{(0)}$ and $\Delta^{(0)}$ have already been obtained from the solution to the $\epsilon = 0$ problem. Inserting equation (28) into the generalized tangency condition and collecting equal powers of ϵ reveals that $Y^{(1)}$ bears the following simple relation to $Y^{(0)}$:

$$Y^{(1)} = \frac{(1 - Y^{(0)})^2}{Y^{(0)}} \cdot \frac{1}{(\mathscr{L} - \mathscr{N}) - 2[1 - Y^{(0)}]} \tag{30}$$

in terms of which

$$\Delta^{(1)} = Y^{(1)} - \frac{(1 - Y^{(0)})^2}{Y^{(0)}\,(\mathscr{L} - \mathscr{N})}. \tag{31}$$

Thus, when ϵ is small, the relative error in Δ due to finite evaporation resistance is simply $\epsilon\, \Delta^{(1)}/\Delta^{(0)}$, which, together with equations (30, 31), can be used to estimate the effects on condensation-enhanced vaporization rates. When ϵ is not small (say, $> 10^{-1}$) the perturbation approach loses its value, and a direct solution of the more general problem is necessary. The effects of ϵ on the dimensionless diffusion layer thickness Δ are illustrated in Fig. 5 for the particular case $\mathscr{S} = 10$. The dashed (small ϵ) behavior is that obtained from the perturbation approach when only linear terms in ϵ are included.

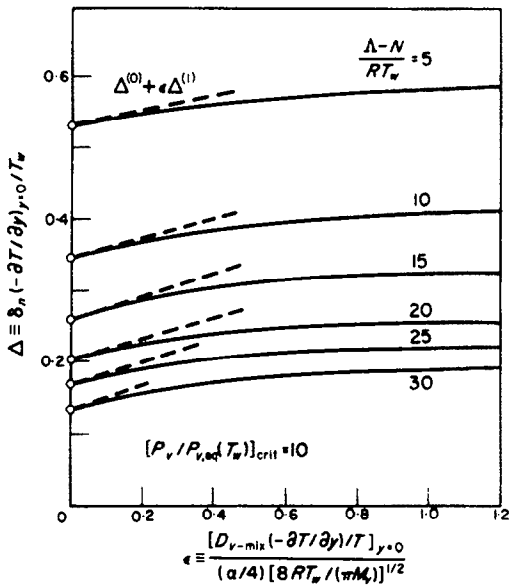

FIG. 5. Effect of interfacial resistance to evaporation on the diffusion boundary-layer thickness in the presence of condensation ($\mathscr{S} = 10$).

4.4.2 *Departures from linear temperature profile* (a, b). If the remaining assumptions underlying the treatment of Section 3 are retained and only (a) and (b) are dropped, the analysis is complicated only in that the position of nucleation must be found in each case from the actual $T(y)$ profile, together with a solution to the source-free diffusion equation in which the tangency condition is imposed as one "boundary" condition. While this can certainly be carried out graphically or numerically for flow configurations of particular interest, one forfeits the ability to obtain results with the generality of those given in Section 3. Limiting

our solutions to the "film theory" case of nucleation within a locally linear temperature profile or to cases in which the condensation enhancement is relatively large (cf. unshaded region of Fig. 3) is, accordingly, the price we have paid for the generality gained. Interestingly enough, only if $Le \approx 1$ is assumption (b) removable, with the quantities Y, Δ being redefined such that equations (6) and (8) remain valid [16].

4.4.3 *Net interfacial mass transfer (Stefan–Nusselt flow) effect* [5, 15]. In the absence of condensation, the net mass transfer effect due to heterogeneous vaporization (or, equivalently, the "moving boundary" effect) is known to be governed by a dimensionless mass-transfer parameter of the form [5]

$$B_{\text{diff}} = \frac{c_{v,eq}(T_w) - c_{v,\infty}}{1 - c_{v,eq}(T_w)} \tag{32}$$

which, in the present case, must be small compared to unity.* Clearly, this is true when the vapor mass fraction at $y = 0$ is itself small compared to unity (i.e. when $M_v p_{v,eq}(T_w) \ll M_{\text{mix}} p$). For an evaporating liquid, however, the approximation degenerates rapidly as one approaches its boiling point at the prevailing pressure (i.e. when $p_{v,eq}(T_w) \to p$, $B_{\text{diff}} \to \infty$). Applied to the Fe(l)/He(g) example (i.e. $M_v = 55{\cdot}95$, $M_{\text{He}} = 4{\cdot}003$) at 1 atm we find that B_{diff} is approximately 10^{-1} near $T_w = 2300°\text{K}$ but is already 1 at $T_w = 2600°\text{K}$. In the present case we therefore conclude that the interfacial mass velocity effect cannot be neglected for surface temperatures much above 2300–2400°K. This implies, of course, that even the $j''_{\text{min}}(T_w)$ prediction must be modified above these surface temperatures.

4.4.4 *Heat of condensation effect on temperature profile.* The reduction in vapor pressure at $y = y_n$ due to condensation must be accompanied by the evolution of heat. If this heat were adiabatically delivered to the "carrier gas", one can readily estimate the temperature rise at this location and compare the result to $T_w - T_n$. In this way we find that when the surrounding gas is monatomic (as in the present example, for which $M_{\text{He}} c_{p,\text{He}} = 5R/2$) the temperature rise due to condensation will be negligible compared to $T_w - T_n$ if

$$\frac{p_{v,eq}(T_w)/p}{\frac{5}{2} \cdot \frac{\Delta}{\mathscr{L}} \left[\frac{(j''/j''_{\text{min}})}{(j''/j''_{\text{min}})^{-1}} \right]} \ll 1. \tag{33}$$

Evaluation of this parameter for the present Fe(l)/He(g) example leads to a conclusion similar to that obtained in Section 4.4.3, viz. predictions above about 2300–2400°K will be in error due to temperature profile modifications associated with the condensation process itself. This numerical example indicates that any self-consistent generalized theory of condensation-enhanced vaporization which accounts for the heat of condensation effect should simultaneously include the Stefan flow effect, and vice versa. But combined treatment of this more general problem is beyond the scope of the present paper.

4.4.5 *Effect of more realistic nucleation kinetic law.* The simplicity of the critical supersaturation model and the existence of $s_{\text{crit}}(T)$ data provide ample justification for first exploiting this approximation in the relatively unstudied area of condensation phenomena within boundary layers (i.e. with molecular transport). However, to gain deeper insight into the nature of the approximations implicit in the critical supersaturation approach and to provide a general formalism suitable for use as more realistic condensation–growth kinetic data become available, studies using classical homogeneous nucleation theory have been initiated [16].

5. CONCLUSIONS

By making a reasonable assumption (c) concerning the form of the critical supersaturation vs. temperature relation, simple analytical expressions [equations (14) and (18)] have been

* When B_{diff} is small, the relative error in j''_{min} due to this cause is about $\frac{1}{2}B_{\text{diff}}$ (cf. [15]).

derived for the enhancement in vaporization rate accompanying nucleation within a thermal boundary layer. These predictions, which focus attention on a minimum number of basic dimensionless parameters, clearly display the physicochemical conditions under which large enhancements in vaporization rates can be expected. It is hoped that the present treatment will facilitate further comparison of this model with experimental data, as well as open the way to further generalizations (cf. Section 4) of practical interest. To guide theoretical developments in this general area of mass transport phenomena, additional experimental data are required for systems which [based on equation (14)] should reveal large enhancements in vaporization rates due to condensation within the thermal boundary layer. In this connection, it should be remarked that analogous behavior is expected in nonisothermal solid–liquid systems (dissolution) as well. Indeed, some of these systems may provide experimental advantages, making their study more accessible and equally fruitful.

ACKNOWLEDGEMENTS

It is a pleasure to acknowledge the extensive computational assistance of A. Crossley in preparing this paper for publication. I also wish to thank Drs. E. Turkdogan, H. Thomann, D. Olander, P. Hill, R. Andres, and W. Courtney for their helpful correspondence.

REFERENCES

1. S. K. Friedlander and M. Litt, Diffusion-controlled reaction in a laminar boundary layer, *Chem. Engng Sci.* **7**, 229 (1958).
2. E. T. Turkdogan, P. Grieveson and L. S. Darken, Enhancement of diffusion-limited rates of vaporization of metals, *J. Phys. Chem., Ithaca* **67**, 1647 (1963).
3. E. T. Turkdogan and K. C. Mills, The theory of enhancement of diffusion-limited vaporization rates by a convection–condensation process, Part II—experimental, *Trans. Am. Inst. Min. Engrs* **230**, 750 (1964).
4. E. T. Turkdogan, The theory of enhancement of diffusion-limited vaporization rates by a convection–condensation process, Part I—theoretical, *Trans. Am. Inst. Min. Engrs* **230**, 740 (1964).
5. D. B. Spalding, *Convective Mass Transfer: An Introduction*. McGraw-Hill, New York (1963).
6. J. P. Hirth and G. M. Pound, Condensation and evaporation, nucleation and growth kinetics, in *Progress in Materials Science*, edited by B. Chalmers, Vol. 2. MacMillan, New York (1963).
7. A. Stodola, *Steam and Gas Turbines*. McGraw-Hill, New York (1927).
8. B. Lewis and G. Von Elbe, Theory of flame propagation, *Proceedings of the Second Symposium on Combustion*, pp. 183–188. The Combustion Institute, Pittsburgh (1937).
9. R. P. Andres, Homogeneous nucleation from the vapor phase, *I/EC Fundamentals* **57**, 24 (1965).
10. R. D. Gretz and J. P. Hirth, Nucleation in surface-catalyzed chemical vapor deposition, presented at the Symposium on Nucleation Rates and Growth Mechanisms (May, 1966), A.I.Ch.E. Preprint 3C.
11. E. R. G. Eckert and R. M. Drake Jr., *Heat and Mass Transfer*, 2nd edn. McGraw-Hill, New York (1959).
12. J. N. Butler and R. Brokaw, Thermal conductivity of gas mixtures in chemical equilibrium, *J. Chem. Phys.* **26**, 1636 (1957).
13. D. E. Rosner, Fundamental solution to the diffusion boundary layer equation for separated flow over solid surfaces at very large Prandtl numbers, *Int. J. Heat Mass Transfer* **6**, 793 (1963).
14. O. Knacke and I. N. Stranski, The mechanism of evaporation, in *Progress in Metal Physics*, Vol. 6. Pergamon Press, London (1956).
15. D. E. Rosner, Effects of the Stefan–Nusselt flow on the apparent kinetics of heterogeneous chemical reactions in forced convection systems, *Int. J. Heat Mass Transfer* **9**, 1233 (1966).
16. M. Epstein and D. E. Rosner, Enhancement of diffusion-limited vaporization by condensation within the thermal boundary layer. II. Effect of Nucleation Kinetics, In preparation.

Résumé—Les conditions générales sous lesquelles la condensation dans la couche limite thermique peut renforcer les vitesses d'évaporation limitées par la diffusion de liquides ou de solides dans des ambiances plus froides sont examinées théoriquement, en se basant sur la notion que la condensation se produit lorsqu'une "sursaturation critique" est obtenue. Des expressions simples sont obtenues pour l'augmentation prévue en fonction de la chaleur de vaporisation sans dimensions Λ/RT_w, de la sursaturation critique évaluée à la température de surface $s_{crit}(T_w) \equiv p_{v,\,crit}/p_{v,\,eq}(T_w)$, et d'un paramètre qui régit la dépendance de s_{crit} en fonction de la température. Ces résultats montrent clairement les conditions thermodynamiques et de transport sous lesquelles de grandes augmentations peuvent être attendues. La facilité avec laquelle ils ont pu être utilisés pour des prévisions absolues et la comparaison avec les données disponibles est illustrée dans le cas de sphères de fer fondu s'évaporant dans de l'hélium au repos à pression atmosphérique.

Zusammenfassung—Es werden die allgemeinen Bedingungen analytisch untersucht, unter welchen die durch Diffusion begrenzten Verdunstungsgeschwindigkeiten von Flüssigkeiten oder festen Stoffen in kälterer Umgebung dadurch vergrössert werden, dass Kondensation innerhalb der thermischen Grenzschicht auftritt. Dabei wird davon ausgegangen, dass die Kondensation dann eintritt, wenn eine "kritische Übersättigung" erreicht ist. Einfache Ausdrücke für die erwartete Geschwindigkeitsvergrösserung werden abgeleitet als Funktion der dimensionslosen Verdampfungswärme Λ/RT_w, der kritischen Übersättigung, ermittelt bei der Oberflächentemperatur $s_{crit}(T_w) = p_{v,crit}/p_{v,eq}(T_w)$ und einem Parameter, der die Temperaturabhängigkeit von s_{crit} berücksichtigt. Diese Ergebnisse zeigen klar die thermodynamischen und die Transportbedingungen, unter denen starke Geschwindigkeitsvergrösserungen erwartet werden können. Die Einfachheit, mit der diese Ergebnisse für absolute Vorhersagen und für Vergleiche mit vorhandenen Daten angewendet werden können, wird demonstriert am Beispiel geschmolzener Eisenkugeln, die bei Atmosphärendruck in ruhendes Helium verdampfen.

Аннотация—На основании допущения, что конденсация происходит при достижении «критического перенасыщения», аналитически исследовались общие условия, при которых конденсация в тепловом пограничном слое может увеличить скорости диффузионного испарения жидкостей или твердых тел в более холодной среде. Выведены простые выражения для ожидаемого увеличения в зависимости от безразмерной теплоты испарения Λ/RT_w, критического перенасыщения, оцененного при температуре поверхности s_{crit} $(T_w) \equiv P_{v,crit}/P_{v,eq}$ (T_w), и параметра, описывающего температурную зависимость s_{crit}. Эти результаты ясно отображают термодинамические условия и условия переноса, при которых можно ожидать большое увеличение темпа испарения. В виде иллюстрации справедливости применения данного метода оценки и совпадения с имеющимися сведениями приводится случай испарения капель жидкого железа в неподвижный гелий при атмосферном давлении.